Journal of *Marine Science and Engineering*

MDPI

Article

An Artificial Intelligence Approach for Coastal Structures Adaptation to Climate Change: Insights from a Case Study in the Mediterranean Sea

Nerea Portillo Juan [1,*], Javier Olalde Rodríguez [1], Vicente Negro Valdecantos [1], Jose María del Campo [1] and Peter Troch [2]

[1] Environment, Coast and Ocean Research Laboratory, Campus Ciudad Universitaria, Universidad Politécnica de Madrid, Calle del Profesor Aranguren 3, 28040 Madrid, Spain; j.olalde@alumnos.upm.es (J.O.R.); vicente.negro@upm.es (V.N.V.); josemaria.delcampo@upm.es (J.M.d.C.)
[2] Department of Civil Engineering, Ghent University, Technologiepark 60, 9052 Ghent, Belgium; peter.troch@ugent.be
* Correspondence: nf.portillo@upm.es

Abstract

The application of artificial intelligence (AI) models in maritime and coastal engineering has gained increasing relevance, demonstrating performance comparable to traditional approaches in wave climate analysis and propagation. However, their use in climate change impact and adaptation studies remains limited, particularly for the design and upgrading of coastal protection structures. To address this gap, this study focuses on the development of an AI-based framework to support the adaptation of breakwaters to future climate conditions. A hybrid approach combining artificial neural networks (ANNs) and genetic algorithms (GAs) was implemented, with two feedforward neural networks-based models developed and applied to different sections of the north breakwater of the Port of Valencia, specifically a vertical section and a compound breakwater. The results indicate that, under future climate scenarios (2050), increases of up to 1.2 m in crest elevation, together with reinforcement of the armor layer, are required to ensure adequate structural performance. The analysis also highlights the critical role of extreme events, as approximately 60% of the model errors were concentrated in the upper 90th percentile of wave conditions. Overall, the proposed hybrid ANN-GA framework demonstrated very strong performance, achieving computational efficiencies 30 to 40 times greater than ANN-only models in terms of computational time. These findings underscore the necessity of adapting coastal structures to climate change and confirm the potential of AI-based models as effective tools for climate-resilient coastal engineering, while emphasizing the importance of accurately representing extreme wave conditions.

Keywords: data-driven models; climate change; structural adaptation; genetic algorithms; artificial neural networks; probabilistic approach

Academic Editors: Dong-Sheng Jeng and Giuseppe Roberto Tomasicchio

Received: 8 January 2026
Revised: 29 January 2026
Accepted: 26 February 2026
Published: 27 February 2026

1. Introduction

The coastal ecosystems and structures are one of the systems most threatened by climate change. Climate change is already provoking damages to properties and structures that protect the coastline, and it is expected that in the upcoming years, extreme events and flooding will become even more frequent and intense [1]. In this context of uncertainty, researchers are putting so much effort into studying how climate change is going to affect

coastal ecosystems in the future. Most of the literature focuses on the effect of climate change on shoreline evolution. However, research on ports and their adaptation to climate change is much less abundant [2].

Within the research domain of climate change and ports, various sub-themes emerge, including assessments of flooding risks, evaluations of port operability, strategic approaches, and studies on coastal structures. Flood studies mostly evaluate the impact of SLR [3–6] and wave overtopping [7–10]. Operability studies assess harbor agitation and siltation, applying Boussinesq-type models [11,12], mild-slope equations models [13,14], and hydrodynamic models [15–17]. Some research papers with a more strategic and political approach can also be found in the study of ports adaptation to climate change [18–22].

Finally, a thematic block concerning the adaptation of coastal structures can be distinguished. Despite being one of the most pressing issues, it remains one of the least discussed topics within the scientific community. Within adaptation of coastal structures to climate change, there are mainly two types of studies: those that assess the performance of different alternatives and those that evaluate the performance of these structures under the context of climate change. The assessment of different alternatives has been carried out by different authors [23–26]. However, referring to the structural and hydraulic adaptation of coastal structures to climate change, there is still much knowledge uncertainty, and the amount of research conducted is scarce compared to the other subfields.

Takagi et al. [27] were some of the first authors to assess the performance of coastal structures under new wave conditions; they applied probability functions to assess the sliding stability of breakwaters. Suh et al. [28] presented a new methodology to incorporate the effect of climate change into the design of breakwaters. Mase et al. [29] applied a probabilistic approach to evaluate the stability of a compound breakwater. Sekimoto et al. [30] were also some of the first researchers to apply a probabilistic methodology to assess the performance of coastal structures under climate change scenarios, and Lee et al. [31] studied the armor stability of inclined coastal structures under SLR. Finally, Sergent et al. [32] also studied the adaptation of coastal structures to climate change, more specifically to sea level rise.

In the last years, some studies have been remarkable. Formentin et al. [33] assessed the hydraulic and structural performance of including crown walls on top of dykes. Allsop, W. [34] presented the cases of the adaptation of two breakwaters in the UK. Radfar, S. and Galiatsatou, P. [35] combined a nonstationary extreme value analysis (NEVA) with a probabilistic approach to carry out a reliability analysis of coastal structures. In the last year, Baldoni et al. [36] studied the adaptation of coastal structures in the Adriatic Sea.

Most of these studies that assess coastal structures adaptation involve the use of complex numerical models [1,37–39]. Although these numerical models are the most advanced and sophisticated tools currently in the field, the associated computational cost is huge, which limits their application.

In the last years, AI models have irrupted in the scientific realm. Data-driven approaches are gaining visibility, and they have shown the ability to outperform traditional methodologies in ocean engineering [40]. However, compared to other fields, the level of AI development in this discipline remains less developed. Primarily, AI technologies have been applied in the prediction and characterization of maritime weather, yielding highly encouraging results [40,41]. However, the presence of AI technologies in coastal structures adaptation studies is almost negligible.

The objective of this paper is to address the gap in applying AI-based methodologies to the adaptation of coastal structures under future climate scenarios, an area that has received limited attention in the literature. This study introduces a novel hybrid framework that

combines level III reliability analysis (Monte Carlo simulations) with ANNs. The approach combines the complementary strengths of both techniques: Monte Carlo simulations generate large, physically consistent datasets of breakwater configurations and wave conditions, while ANNs efficiently learn and generalize from these data.

The ultimate goal is to provide a practical and computationally efficient methodology to support the adaptation of coastal structures to climate change, significantly reducing the cost and time compared to full numerical models. The proposed framework is intended as a preliminary decision-support tool, suitable for exploratory analyses, sensitivity studies, and comparison of adaptation strategies across a wide range of future wave climates. Its application with experimental and in situ field data represents a necessary next step for further validation and refinement; however, such data were not available for the considered structures and climate scenarios at the time of this study. This limitation is explicitly acknowledged, and future work is recommended to address it in order to enhance confidence in design applications.

The proposed framework provides added value by efficiently generalizing established design knowledge across a high-dimensional parameter space. This enables a rapid and systematic exploration of breakwater adaptation strategies under a wide range of future wave climates, something that is difficult to achieve using conventional approaches alone.

The proposed model was tested in Port of Valencia using two sections of the north breakwater. These years were chosen because they represent mid-term planning horizons commonly used in climate change adaptation studies, allowing assessment under plausible near-future scenarios. Longer-term horizons, such as 2100, were not considered, as doing so would reduce reliability and could be overly optimistic given the uncertainties involved. Since this is a novel approach applying Monte Carlo simulations to structural adaptation, focusing on 2035 and 2050 provides a more robust and conservative assessment.

2. Materials and Methods

This section is divided into three subsections. Section 2.1. focuses on the characterization of wave climate. Section 2.2. explains the characterization of coastal structures. Finally, Section 2.3. presents the AI model, a hybrid AI model that applies genetic algorithms (GAs) and artificial neural networks (ANNs). Figure 1 shows the workflow of the methodology.

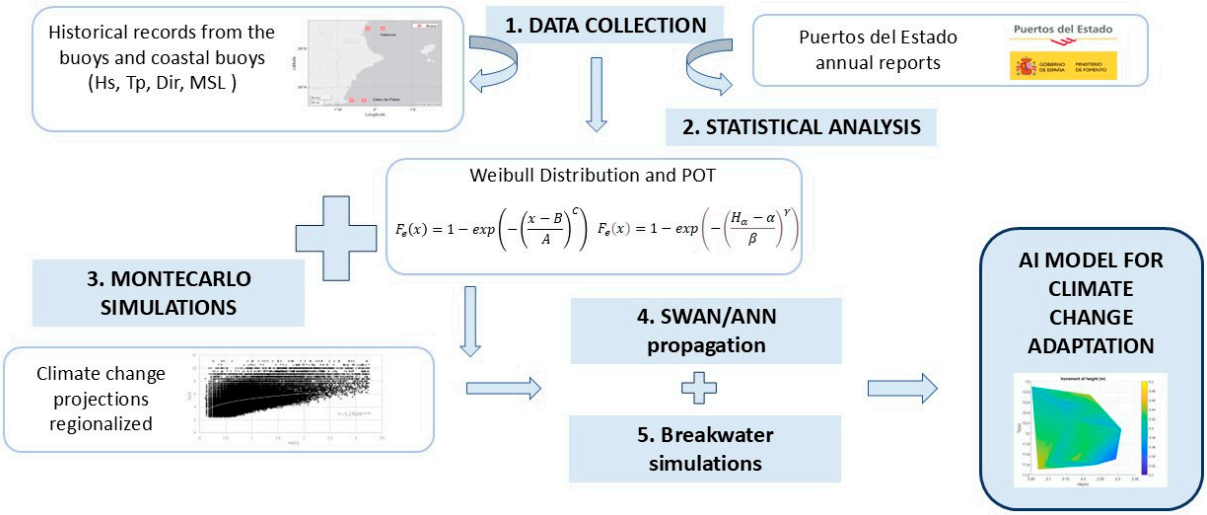

Figure 1. Methodology.

The first step of the study involved conducting a statistical and correlation analysis to fully characterize the wave climate in Valencia. Secondly, data on all the breakwaters

along the Spanish Mediterranean Sea was collected. With the wave climate propagated to the toe of the structure and the breakwater characterized structurally, geometrically, and hydraulically, both databases were combined. Finally, the safety coefficient and the adaptation measures required of the breakwater sections for each of the cases were calculated. After completing these calculations, all the requisite sets of inputs and outputs to construct and train the AI model were obtained.

2.1. Study Area and Data

The area of study is the port of Valencia, Spain, which is in the Western Mediterranean (Figure 2). The orography of this area makes the Western Mediterranean subject to local meteorological processes with wave and wind patterns that are difficult to characterize in global models. It is also one of the areas that is most affected by climate change and where it is expected to have the greatest impact at a social and economic level. Despite its vulnerability, the area remains underrepresented in climatological studies. Remarkably, neighboring regions have garnered more significant attention, overshadowing the need for focused investigations in Valencia [42].

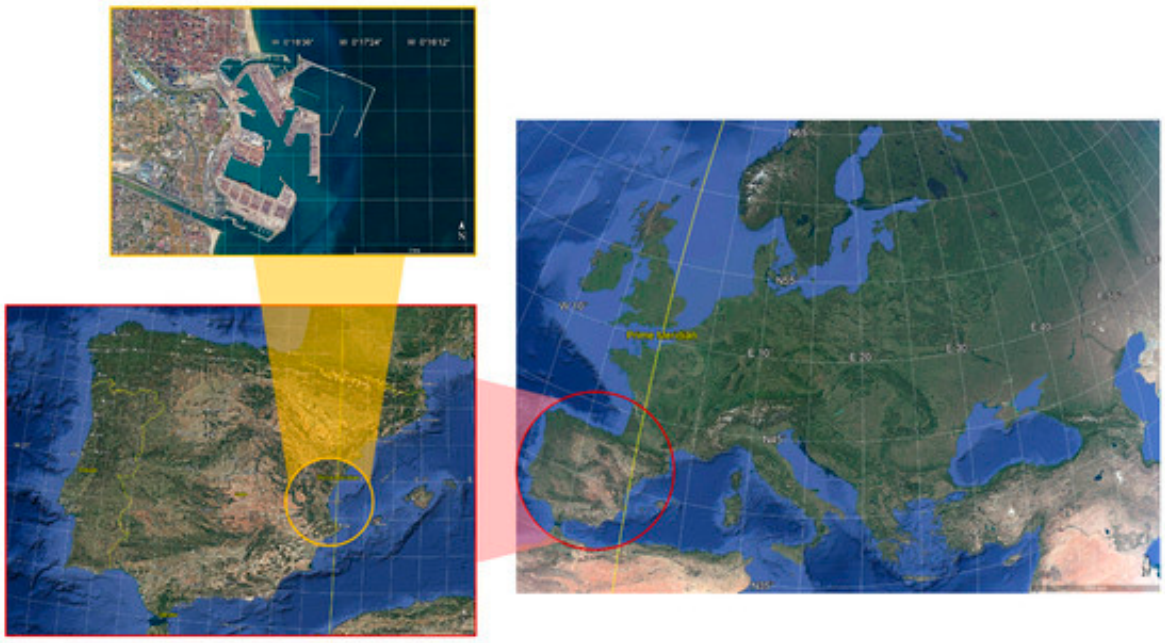

Figure 2. Area of study—Valencia.

For this study, the data of the Spanish authority in charge of wave climate and the management of ports were used [43]. Hourly significant wave height (H_s), peak period (T_p) and Direction (Dir) records from the Valencia buoy and the coastal Valencia buoy were taken. Detailed information regarding the study area, buoy locations, and wave databases is provided in our previous publication [40], including coordinates and full references, and is therefore not repeated here to avoid redundancy. Wave propagation from deep water to the breakwater toe was performed using both numerical simulations with SWAN and AI-based models (ANNs), as described in [40], with both approaches producing comparable results.

Once the data were collected, a thorough study and evaluation of the trends in wave climate was conducted. The parameters of the wave distributions and their evolution over the historical series were analyzed. This analysis is presented in Figure 3, which illustrates the historical evolution and distribution of the records. Additionally, the scatter diagrams of H_s and T_p were examined, which are depicted in joint plots alongside the histograms for Valencia (Figure 4).

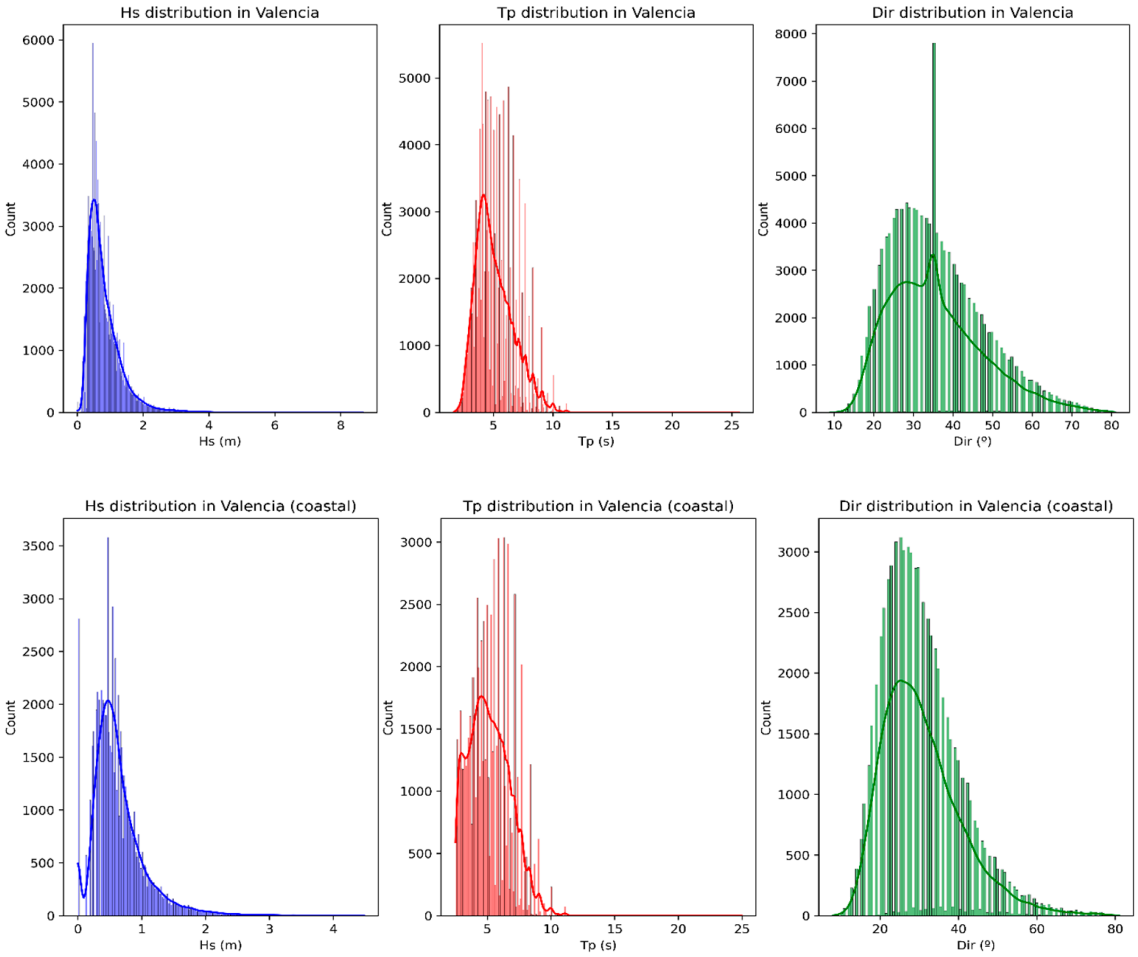

Figure 3. Histogram and distribution of wave data records in Valencia.

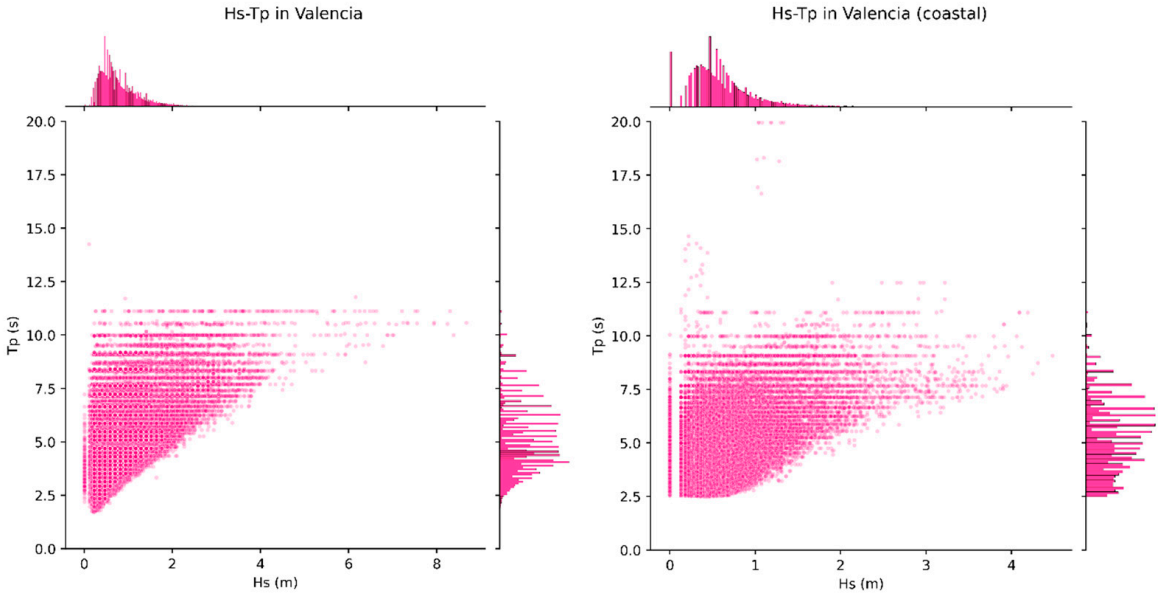

Figure 4. Joint plots of Valencia.

Finally, a thorough seasonal analysis was performed to identify and understand the variations in wave patterns across different times of the year. Additionally, an outliers analysis was conducted to detect and examine any anomalies in the wave data (Figure 5). In the figure, it can be appreciated how most of the outliers are concentrated in winter.

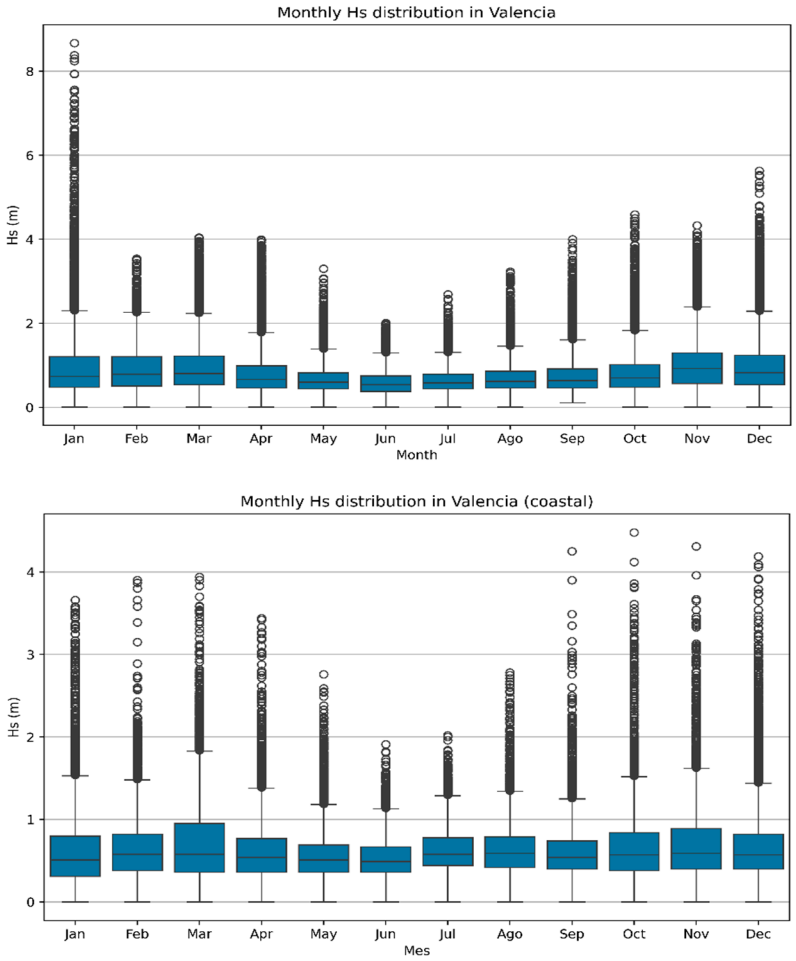

Figure 5. Seasonal and outliers' analysis.

2.2. Coastal Structure Characterization

After propagating the wave climate to the breakwater toe, the coastal structures were characterized. For this purpose, information from all the breakwaters along the Spanish Mediterranean coast was compiled. A total of 18 breakwaters, which are the total of breakwaters that are located in the Levantine area, were studied [44].

As the model was applied to the specific case of the north breakwater of the Valencia port, whose two most critical sections are a compound breakwater (end of the trunk) and a vertical breakwater (head of the breakwater), only data on vertical and compound breakwaters were collected (Tables 1 and 2).

Table 1. Statistical study of the values of the main variables of compound breakwaters in the Spanish Mediterranean Sea.

Variable	[Min, Max]	[μ, σ]
h	[13.75, 45]	[30.15, 12.48]
d	[0, 26.4]	[9.64, 11.22]
h'	[5.5, 28]	[15.5, 9.01]
h_c	[1, 3]	[2.00, 0.58]
R_c	[1.75, 13]	[7.75, 3.99]
A	[6, 24.1]	[16.7, 8.27]
W_m(t)	[9990, 72,829]	[43,196, 25,984]
W_{50}(t)	[0.50, 70]	[15.2, 30.64]

Table 2. Statistical study of the distribution of the main variables of vertical breakwaters in the Spanish Mediterranean Sea.

Variable	[Min, Max]	[μ, σ]
h	[12, 48]	[21.72, 10.42]
d	[8.4, 26.4]	[14.1, 5.06]
h'	[10, 28]	[16.03, 4.99]
h_c	[1, 3]	[2.00, 0.58]
R_c	[5.7, 13]	[9.9, 2.45]
W (t)	[5116, 139,200]	[50,063, 36,226]
A*	[6.89, 67.6]	[30.85, 19.3]

* The width of double caissons was also considered.

Once all the coastal structures' characteristics were defined, a probabilistic characterization of the breakwaters using Monte Carlo simulations was conducted, following the same approach that was applied in the wave climate characterization. In order to carry out the Monte Carlo simulations, a uniform distribution for each of the main variables of each section was defined, with values between the maximum and minimum values of the breakwaters in the Spanish Mediterranean area (Tables 1 and 2).

For the compound breakwater (Table 1), the main variables selected were the design water depth (h), the distance from the berm to the Mean Sea Level (MSL) (d), the distance from the bedding layer to the MSL (h'), the distance between the monolith crest elevation and the MSL (h_c), the freeboard (R_c), the specific weight of the blocks (γ), the weight of the breakwater (W_{50}), the width of the monolith (A), the weight of the monolith (W_m), and the maximum admissible overtopping (q_{max}).

For the vertical breakwater (Table 2), the main variables selected were the design water depth (h), the distance from the berm to the Mean Sea Level (MSL) (d), the distance from the bedding layer to the MSL (h'), the distance between the monolith crest elevation and the MSL (h_c), the freeboard (R_c), the weight of the breakwater (W), the width of the monolith (A), and the maximum admissible overtopping (q_{max}).

Before conducting the Monte Carlo simulations, an in-depth statistical analysis of the existing correlations among the key variables was undertaken (Figures 6 and 7); d, h′, and h were highly correlated. Therefore, only the variable h was used to feed the ANN model.

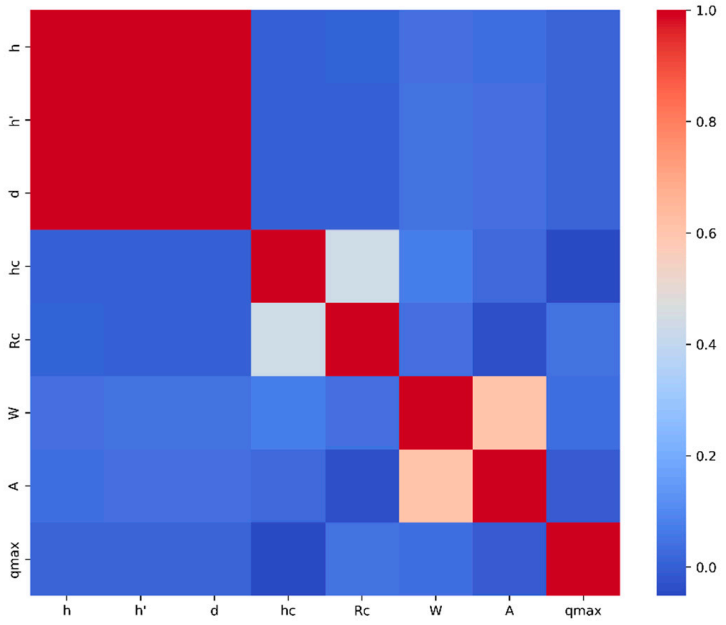

Figure 6. Correlation heatmap for the vertical breakwater.

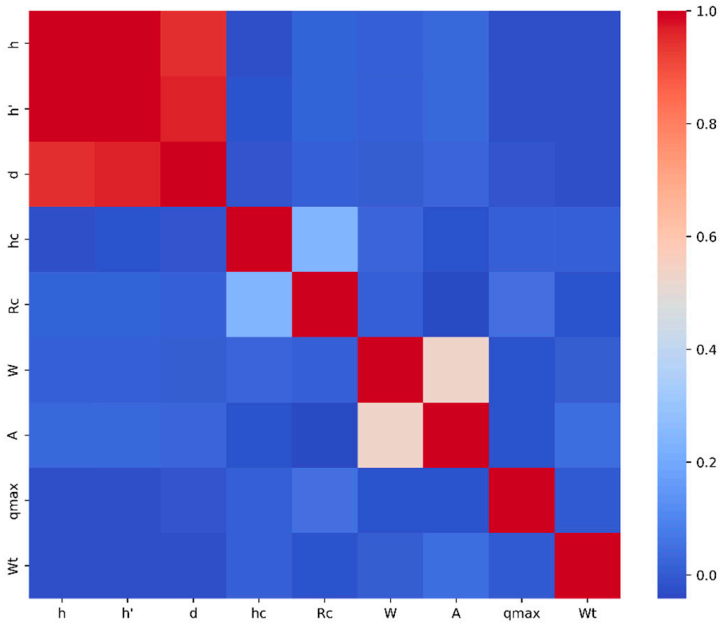

Figure 7. Correlation heatmap for the compound breakwater.

A total of 1000 simulations were executed, each representing diverse breakwater arrangements and configurations. It is important to emphasize that all the simulations were filtered, eliminating configurations of breakwaters that lacked coherence or practicality. This approach aimed to generate a statistically representative sample encompassing various scenarios across the Spanish Mediterranean. The filtering of the breakwater configurations was based on physical parameters, doing the following checks: (1) h > h′; (2) h > d; (3) W > 600A; (4) W < 2100A. These constraints implicitly preserved the physical correlation between parameters such as h, d, and h′, as all variables were sampled within bounded ranges derived from conventional design practice and subsequently validated through the same set of coupled conditions.

After filtering, the resulting set of structurally consistent breakwater configurations was combined with the maritime climate conditions obtained from the wave climate database described in Section 2.1. Each valid structural configuration was paired with all relevant wave climate scenarios, assuming independence between structural geometry and external forcing, which is appropriate for adaptation analysis under future climate projections. The integration of both datasets was performed using a dedicated Python 3.12 routine that systematically merged all compatible combinations, leading to a final dataset of 2×10^6 different cases.

Equations for Evaluating Structural Performance

Once all the scenarios for various breakwater configurations and wave conditions were defined, the structural performance of the breakwater was assessed across these different cases.

In the case of the compound breakwater, the Sliding Safety Coefficient of the monolith (SSD), the block damage (N_{od}), and the overtopping (q) were computed. In the case of the vertical breakwater, the SSD and the q were obtained.

The design wave height was defined following Goda formulae (Equations (1)–(3)) [27,45,46]

$$H_D = mín(H_b, H_{max}) \quad (1)$$

$$H_{max} = H_{1/250} \cong 1.8H_s \quad (2)$$

$$H_b = 0.17 L_0 \left\{ 1 - exp\left[-1.5 \frac{\pi h}{L_0} (1 + 15 \tan\theta^{4/3}) \right] \right\} \quad (3)$$

where L_0 is the wavelength in deep water and $\tan\theta$ the slope of the ground.

For the calculation of the block damage N_{od}, the Van der Meer formula was used (Equations (4)–(6)) [47]

$$\frac{H_s}{\Delta D_{n50}} = \left(6.7 \frac{N_{od}^{0.4}}{N^{0.3}} + 1 \right) s_m^{-0.1} \quad (4)$$

$$s_m = \frac{2\pi H_s}{g T_{m,0}^2} \quad (5)$$

$$\Delta = \left(\frac{\gamma}{\gamma_w} - 1 \right) \quad (6)$$

where γ is the specific weight of the blocks, γ_w is the specific weight of water, N is 1000 waves for the Mediterranean Sea, and $T_{m,0}$ is the mean zero-crossing wave period.

To calculate the sliding safety coefficient of the monolith, the Goda–Takashi wave load formula was applied [48]. The wave height used to calculate the sliding safety coefficient was the transmitted wave height (H_t) through the armor (Equations (7) and (8)) [49]

$$c_t = 0.46 - 0.3 \frac{R_c}{H_s} \quad (7)$$

$$H_t = c_t H_s \quad (8)$$

Finally, for the overtopping, the EurOtop manual [50] and Franco et al. [51] formula were used (Equation (9)).

$$\frac{q}{\sqrt{g H s^3}} = 8 \times 10^{-5} \exp\left(3.10 \left(\frac{R u_{\xi 0}^{2\%} - Rc}{Hs} \right) \right) \quad (9)$$

where $Ru_{\xi 0}^{2\%}$ is defined as a function of the number of Iribarren ξ [52] (Equations (10) and (11)).

$$Ru_{\xi 0}^{2\%} = a\xi \; if \; \xi < 1.5 \quad (10)$$

$$Ru_{\xi 0}^{2\%} = b\xi^c \; if \; \xi > 1.5 \quad (11)$$

For the vertical breakwater, the following formulas and equations were used.

The design wave height was defined following Goda formulae (Equations (1) and (2)) [27,45,46].

The Goda–Takashi wave load formula [48] was used to compute the loads on the vertical breakwater (Equations (16)–(19)).

To calculate the pressure, first, the auxiliar parameters α_1, α_2, and α_3 must be defined (Equations (12)–(14))

$$\alpha_1 = 0.60 + \frac{1}{2} \left[\frac{\frac{4\pi h}{L}}{\sin \frac{4\pi h}{L}} \right]^2 \quad (12)$$

$$\alpha_2 = \min\left(\frac{h_b - d}{3 h_b} \left(\frac{H_D}{d} \right)^2, \frac{2d}{H_D} \right) \quad (13)$$

$$\alpha_3 = 1 - \frac{h'}{h} \left(1 - \frac{1}{\cosh \frac{2\pi h}{L}} \right) \quad (14)$$

Once α_1, α_2 and α_3 were defined, the pressure on the breakwater was calculated (Equations (16)–(19)).

Where β is the incident wave direction, ρ_w is the water density, g is the gravity, and η is the wave run-up (Equation (15)).

$$\eta = 0.75(1 + \cos\beta)H_D \tag{15}$$

$$P_1 = \frac{1}{2}(1 + \cos\beta)\left(\alpha_1 + \alpha_2 \cos\beta^2\right)\rho_w g H_D \tag{16}$$

$$P_2 = \frac{P_1}{ch2\pi\frac{h}{L}} \tag{17}$$

$$P_3 = \alpha_1\alpha_3\rho_w g H_D \tag{18}$$

$$P_4 = \frac{\eta - h_c}{\eta}P_1 \tag{19}$$

Figure 8 shows the diagram of the pressures, P_1, P_2, P_3, and P_4. For the forces, the pressure area was integrated.

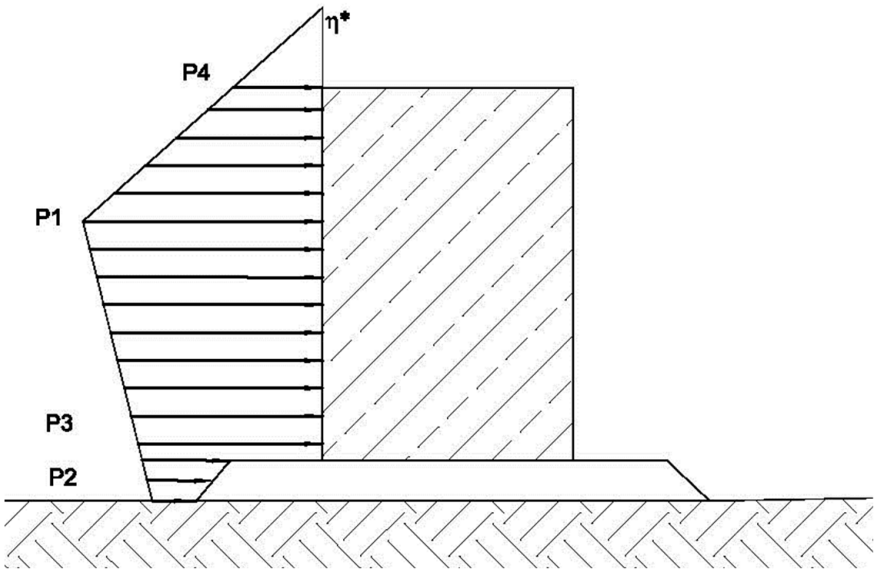

Figure 8. Pressure diagram on a vertical breakwater taken from [53].

To calculate the safety coefficient for sliding, the Goda equation was also used [54] (Equation (20)).

$$C_{SD} = \frac{\sum \delta F_v}{\sum F_H} = \frac{0.6(W_{50} - p_u)}{\sum F_H} \tag{20}$$

where p_u is the uplifting pressure, C_{SD} is the sliding safety coefficient, W_{50} is the average weight, and F_H are the horizontal forces.

To calculate the overtopping, and the maximum admissible overtopping, the EurOtop manual [50] and Franco et al. [51] formula were used (Equation (21)).

$$\frac{q}{\sqrt{gHs^3}} = 0.082\exp\left(-3\frac{R_c}{H_s}\right) \tag{21}$$

Finally, to define the adaptation measures for both the vertical and the compound breakwater, the required crest height increase needed to meet the prescribed safety coefficients, and limit overtopping was determined. Once these calculations were completed, all the necessary input and output sets for building the AI-based model were available. Table 3 shows the inputs and the outputs parameters for the vertical and compound break-

water, where CB means Compound breakwater and they are parameters that were added in the CB model.

Table 3. Inputs and outputs of the AI model.

In/Out	Parameters and Definition
Inputs	1. H_s—Wave height 2. T_p—Peak period 3. *Dir*—Wave direction 4. h—design water depth 5. h_c—distance to MSL 6. R_c —freeboard 7. A—width of the monolith 8. W/W_{50}—weight 9. q—overtopping 10. q_{max}—max overtopping 11. W_m—monolith weight (CB)
Outputs	1. SSC—Sliding Safety Coefficient 2. ΔHeight 3. ΔWeight (CB)

2.3. AI-Based Model

Artificial neural networks (ANNs) are data-driven models that try to mimic the human brain and are made of different layers that pass the information from the first (input) layer to the last (output) layer [55]. They are particularly recommended when the relationship between input–output pairs is known and intricate, as is the case with the problem presented [40].

The original dataset was pre-processed [56]. The number of positive cases (study cases in which structural adaptation was needed) was much lower than the number of negative cases (study cases in which structural adaptation was not needed). Given the very large number of cases (approximately 2 million per breakwater section), the dataset was adjusted using an undersampling approach. Cases in which no structural adaptation was required were selectively filtered out until a balanced dataset was achieved, with equal representation of breakwaters requiring adaptation and those that did not, resulting in a 50–50 proportion. This threshold was chosen to prevent model bias toward the majority class and to ensure that the ANN could learn to reliably distinguish between adapted and non-adapted cases. In the end of the preprocessing, a dataset with 141,660 different cases for the vertical breakwater and 221,257 cases for the compound breakwater models were obtained, which is well above the minimum required to train ANNs [41].

A feedforward neural network (FFNN) was applied, as they are the ANNs that have shown the best performance in modelling ocean engineering problems [41]. A shallow FFNN with one hidden layer was chosen to avoid a high computational cost and the overfitting of the model. The transfer functions were the hyperbolic tangent sigmoid (Equation (22)) for the first layer and the linear transfer function for the last layer (Equation (23)).

$$F(x) = \frac{e^x - e^{-x}}{e^x + e^{-x}} \quad (22)$$

$$F(x) = x \quad (23)$$

The algorithm used was the Levenberg–Marquardt (LM) as it is usually the most efficient algorithm to model ocean and coastal engineering problems [40,41].

The number of hidden neurons was optimized using a Matlab code (R2025b) [57]. Different architectures were tested, using the Relative Mean Square Error (RMSE) as the loss function (Equation (24)). For the optimization of the architecture, a maximum RMSE

value of 0.6 was required for the SSC, 0.3 m for the height increase, and 0.6 t for the weight increase. As a loop termination criterion, it was established that the error would increase for more than 3 iterations in a row, which in turn exceeded the maximum local error of previously tested networks.

$$RMSE = \sqrt{\frac{1}{n}\sum_{i=1}^{n}(o_i - u_i)^2} \quad (24)$$

Finally, 50 different architectures were tested for the vertical breakwater, finding the optimum value at 47 hidden neurons, and 48 architectures were tested for the compound breakwater, finding the optimum value at 39 hidden neurons.

Once the architecture of the model was defined, the weights of the ANN model were optimized using genetic algorithms (GAs). The concept of GAs was firstly introduced by Holland, J.H. [58], and it is based on the nature theory of Darwin. This translated into GA theory means that the characteristics that better fit to the fitness functions are the ones that prevail. In this algorithm, there are three main elements; the parameters of the model (chromosomes); the fitness function, and the biological-inspired operators [59].

The fitness function is the function that evaluates the quality of the parameters. For the process of selecting the best parameters of the model, three main operators are used; crossover, which combines different sets of data creating a new generation of data; mutation, which produces a random change in the data, and selection, which evaluates the best dataset and selects the ones with the highest scores [60,61].

For the GA, a population size of 200 was chosen, with a maximum number of iterations of 100, a crossover percentage of 80%, and a mutation percentage of 20%, and the selection function employed was the roulette wheel selection (Equation (25)).

$$p_i = \frac{f_i}{\sum_{j=1}^{N} f_j} \quad (25)$$

where p_i is the probability of choosing a chromosome i for the next generation, f_i is the fitness of i, and N is the size of the current generation.

With these sets of values, both ANNs were optimized. The final training and validation errors (RMSE) and correlation coefficients (r) are presented in Table 4.

Table 4. Errors of the ANN-GA models.

	Vertical Breakwater Model		**Compound Breakwater Model**		
	SSC	**ΔHeight**	**SSC**	**ΔHeight**	**ΔWeight**
r	0.986			0.874	
RMSE training	0.45	0.19 m	0.53	0.15 m	0.52 t
RMSE validation	0.44	0.19 m	0.53	0.15 m	0.55 t

3. Results

The main characteristics of the models are presented in Table 5. Once the ANN-GA models had been designed and optimized, they were applied to the case of the north breakwater in the Port of Valencia, assessing several wave scenarios projected for 2035 and 2050. The two most critical sections of this structure were chosen for the analysis: the end of the trunk, known as stretch 4, and the head of the breakwater.

Table 5. Model characteristics.

Model Characteristics	Vertical Breakwater	Compound Breakwater
	ANN	
Architecture	[10-47-2]	[11-39-3]
Algorithm	Levenberg–Marquardt	Levenberg–Marquardt
Transfer functions	Sigmoidal and linear	Sigmoidal and linear
Nº epochs	100	100
Learning rate	0.001	0.001
Regularization	Early Stopping	Early Stopping
Data partitioning	Random 70-15-15	Random 70-15-15
Loss function	RMSE and MSE	RMSE and MSE
Output	SSC, Increment of height	SSC, Increment of height, Increment of weight
Validation strategy	Hold-out	Hold-out
	GA	
Nº of iterations	100	100
Population size	200	200
Crossover percentage	80%	80%
Mutation percentage	20%	20%
Selection function	Roulette wheel	Roulette wheel
Normalization of the data	Yes	Yes

The two main sections were tested in the two main modes of failure, sliding, and overtopping, and in the case of the compound breakwater, the block damage (N_{od}) was also computed.

Finally, for the definition of the adaptation measures, the needed increase of height and weight to meet the safety coefficients and to limit the overtopping of the breakwater to the maximum allowable overtopping in the port of Valencia were calculated.

The sections examined appear in Figure 9, which shows the compound breakwater at the end of the trunk, and in Figure 10, which shows the vertical breakwater at the head. In both figures "sección tipo" means section type.

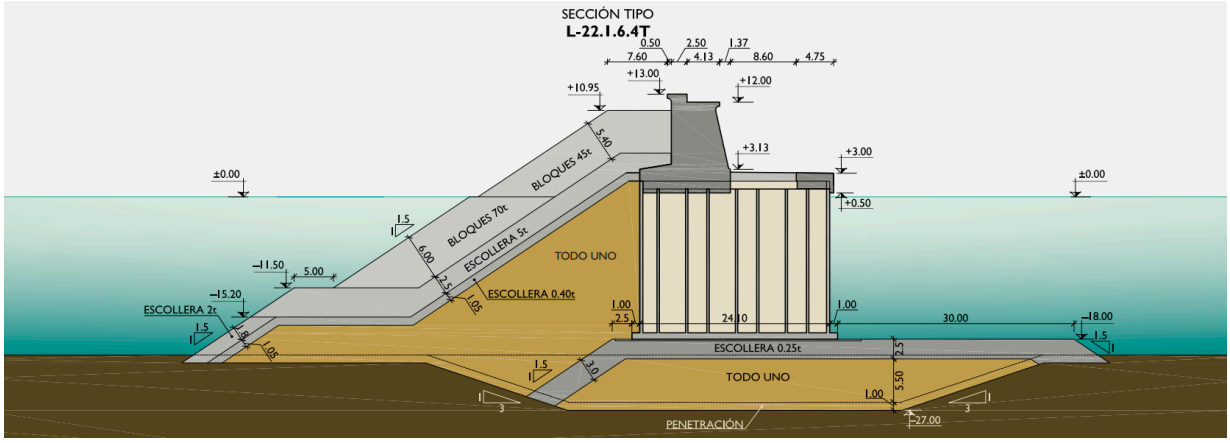

Figure 9. Trunk section. Taken from [44].

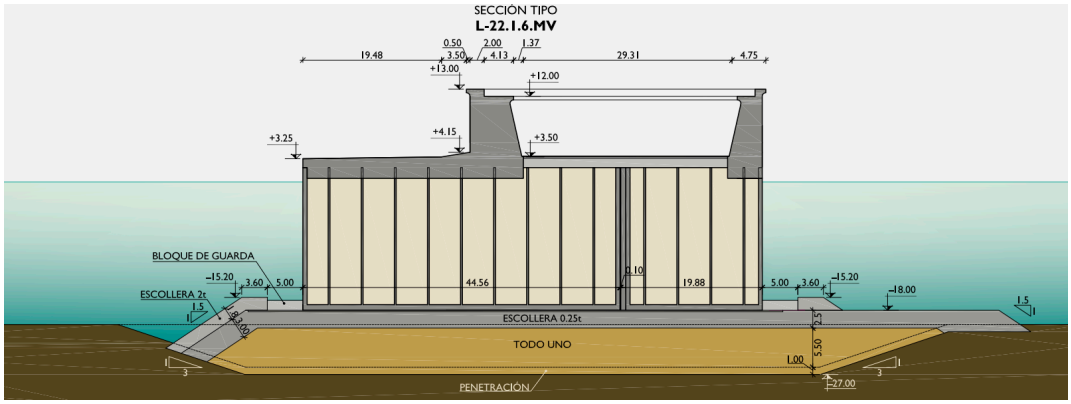

Figure 10. Head section of the north breakwater. Taken from [44].

3.1. Case Study of Valencia Port

As in the whole paper, a probabilistic approach was adopted, subjecting the model to diverse wave conditions encompassing varying wave heights, periods, and directions projected for 2035 and 2050.

The design conditions of the north breakwater for both sections were H_s = 6.84 m and T_p = 7.44 s [44] for a return period of 475 years. A range of wave states corresponding to a return period of 475 years within the timeframes of 2035 and 2050 were systematically analyzed and applied to the ANN-GA model to obtain the adaptation measures needed of the head and fourth stretch-trunk section of the north breakwater in Valencia Port.

When evaluating the safety factors for sliding, both sections met the criteria with a significant margin of safety. Therefore, in this section, only the other two variables (the required increase in height and the weight increment of the slope in the case of the compound breakwater) will be analyzed.

Figure 11 shows the increase in vertical breakwater height required to meet the design conditions, expressed as a function of projected wave height and period. This increase ranges from 0 m under the initial design conditions to 1.2 m in scenarios with higher waves and longer periods. The figure highlights the strong sensitivity of vertical breakwaters to wave period. Pressures, forces, transmission, and other phenomena that govern their behavior depend heavily on this parameter. Even when wave heights are moderate, relatively long periods can demand substantial rises in seawall crest height.

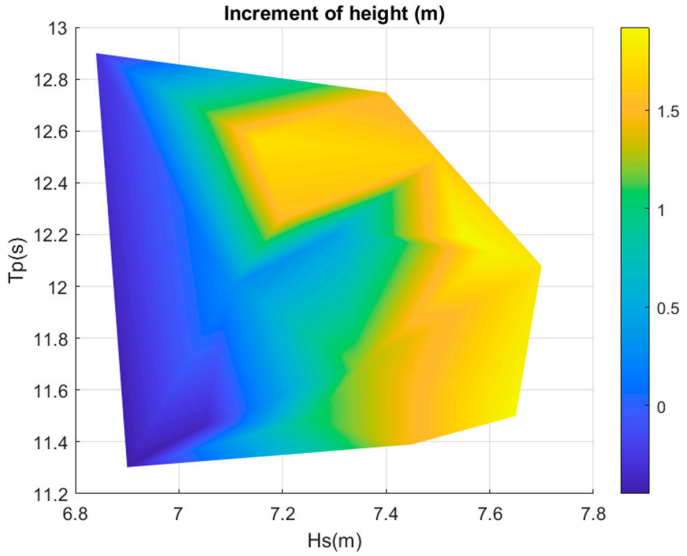

Figure 11. Increment of height for the vertical breakwater for 2035 and 2050.

Figure 12 illustrates the analogous scenario for the compound breakwater. In this instance, the transmitted wave height of the breakwater is depicted on the x-axis. Per the figure, increase of height of the compound breakwater varies much less with wave conditions maintaining a consistently lower value (approximately 0.4 m in all cases). Similar to the vertical breakwater, the wave period plays a pivotal role in shaping the design of a compound breakwater. Careful consideration of wave period is imperative for their adaptation too, particularly when dealing with longer periods coupled with medium waves.

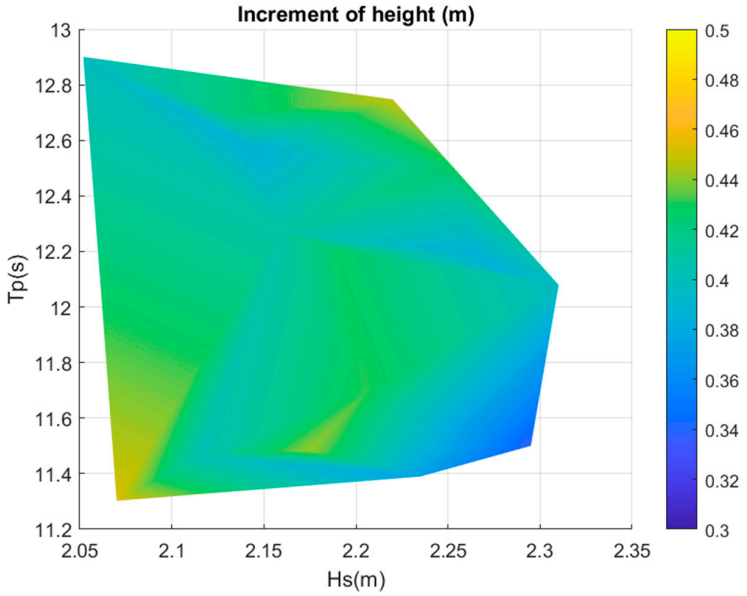

Figure 12. Increment of height for the compound breakwater for 2035 and 2050.

In Figure 13, the incremental weight required to meet safety standards is depicted, determined through the computation of the variable block damage N_{od}. Depending on the prevailing wave conditions, adjustments to the compound breakwater may necessitate weight increases of up to 1 t. Again, especially critical are large wave heights and high periods, as illustrated by the yellow area in the upper right corner of the figure.

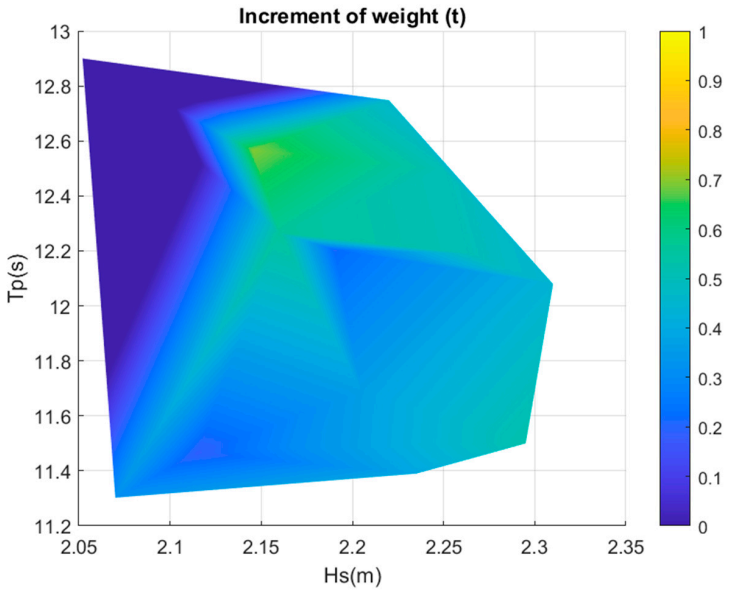

Figure 13. Increment of weight for the compound breakwater for 2035 and 2050.

The outcomes derived from the application of the two models to the Port of Valencia underscore the need for developing adaptation plans of coastal structures to climate changes. They can serve as preliminary design recommendations, which can then be refined and verified using established engineering formulas, codes, and safety criteria. Noteworthy events such as Storm Emma in 2018, Gloria in 2020, and Filomena in 2021 emphasize the critical importance of aligning our structures with evolving climate conditions. With extreme storms growing in frequency and intensity annually, the associated economic and social repercussions are escalating. To avert more severe consequences, it is essential to conduct complete studies of structures situated along the Mediterranean coast. This study reveals the need to increase the crown height by up to 1.2 m in the north breakwater (head section) of the Port of Valencia and augment the weight of the compound section. Implementing these adaptation measures requires an examination of various options, necessitating a detailed study of the Valencia area. The different alternatives span from increasing the breakwater's crown height and adding more blocks to the armor to constructing a reef-breakwater or exploring nature-based solutions such as the utilization of seagrass meadows, which yield equivalent effects. Future research lines should focus on scrutinizing these diverse alternatives, discerning the optimal one within the design constraints of the Valencia Port.

3.2. AI Models Insights and Guidelines

Data-driven models and AI techniques remain notably limited in coastal and ocean engineering studies, particularly in the realm of coastal adaptation research. While AI methodologies are more commonly employed for predicting wave climate, their application in the context of structural adaptation is sparse. After developing two new models, valuable insights can be drawn.

Both models have demonstrated commendable performance, showing low error rates and high correlation coefficients. This is particularly noteworthy as it significantly reduces the computational cost compared to the established numerical models used for coastal structures studies. Nonetheless, certain considerations warrant attention.

Above all, the need for broader and higher-quality datasets grows as the complexity of the modelled process increases. Predicting or propagating maritime climate conditions is relatively simple, since it involves few variables and allows efficient and accurate models to be built with modest datasets. The situation changes when addressing more complex tasks such as structural studies. These models depend on many variables, which makes the process harder to capture and reduces accuracy, even when advanced AI methods are used. A comparative analysis between the current study and the previous investigation focused on maritime climate propagation in the same area [40] reveals two primary observations: a significant escalation in the computational cost (around 100 times more) and a marginal decrease in accuracy (loss of correlation coefficients around 0.1).

Similar contrasts emerge when comparing the models developed for the vertical breakwater and the compound breakwater. Notably, the compound breakwater model exhibits inferior results (r of 0.87 compared to 0.98 for the vertical breakwater) despite utilizing a larger dataset (221,257 data samples compared to 141,660 for the vertical breakwater). Furthermore, the compound breakwater model necessitated more time for training, validation, and testing. This also may be due to the complexity of the modelled process, because the structural and hydraulic behavior of a compound breakwater is usually more complex than that of a vertical breakwater and, consequently, extracting the relationships between the variables that are used as input and the final output of the ANN is more difficult and requires more information and data to arrive at a consistent model.

The computational cost of the model concerning the quantity of input parameters employed was also studied. The increase of computational cost of the ANN with the rising complexity of the modelled process and the associated variables involved highlights the importance of correctly selecting only the essential input variables. It was shown that incorporating only one input more can lead to a substantial increase in computational time, ranging from 15% to 50%, contingent on factors such as the number of epochs and the specific characteristics of the ANN (Figure 14). Therefore, to mitigate unnecessary computational expenses, it is imperative to conduct a sensitivity and correlation analysis before developing any ANN model to discern which variables are necessary to model the process and which can be ignored.

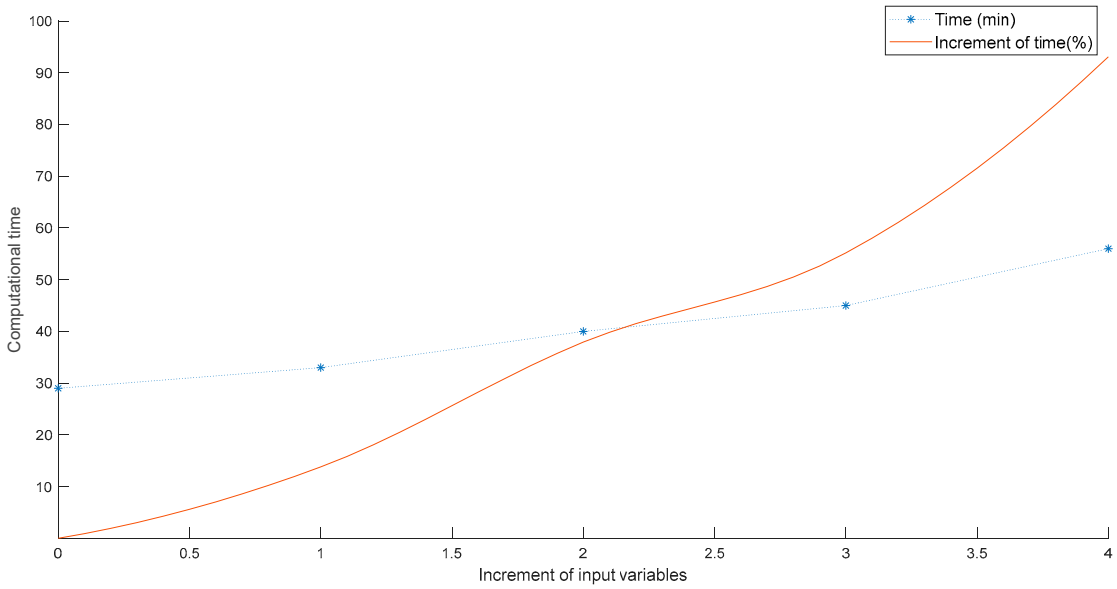

Figure 14. Increment of computational time with the increment of inputs (100 epochs).

Referring to the use of hybrid-AI models, incorporating AI techniques and optimization algorithms, such as GAs, is highly advantageous for minimizing computational time and improving model performance. The implementation of a hybrid model resulted in a remarkable reduction in computational time up to 30–40 times, contingent upon the number of iterations, compared to the conventional trial-and-error approach.

Analysis of model errors shows that most inaccuracies occur under extreme wave conditions. For instance, in the compound breakwater, nearly 60% of the accumulated RMSE is concentrated in the 90th percentile (Figure 15). This pattern is common in data-driven models, which struggle to extrapolate to underrepresented extreme cases. From a design perspective, this limitation means that the model may overestimate or underestimate the adaptation measures needed for rare but critical events. While the framework reliably guides adaptation under typical and moderate conditions, caution is required for extreme scenarios, which are most relevant to structural safety. Future research should focus on improving predictions for these extremes, through enhanced data representation, preprocessing, or integration with experimental and field observations.

Regarding the applicability of the AI-based framework beyond the Port of Valencia, the proposed methodology is broadly transferable to other ports and coastal structures. The core framework, combining Monte Carlo simulations with ANNs, can be applied to any breakwater system to explore structural adaptation under future climate scenarios. However, the model must be carefully calibrated and fine-tuned for each specific site to accurately capture local conditions, including wave climate, bathymetry, breakwater geometry, and structural characteristics. Site-specific adjustments are essential to ensure

that the generated datasets reflect realistic scenarios and that the ANN can learn physically consistent relationships.

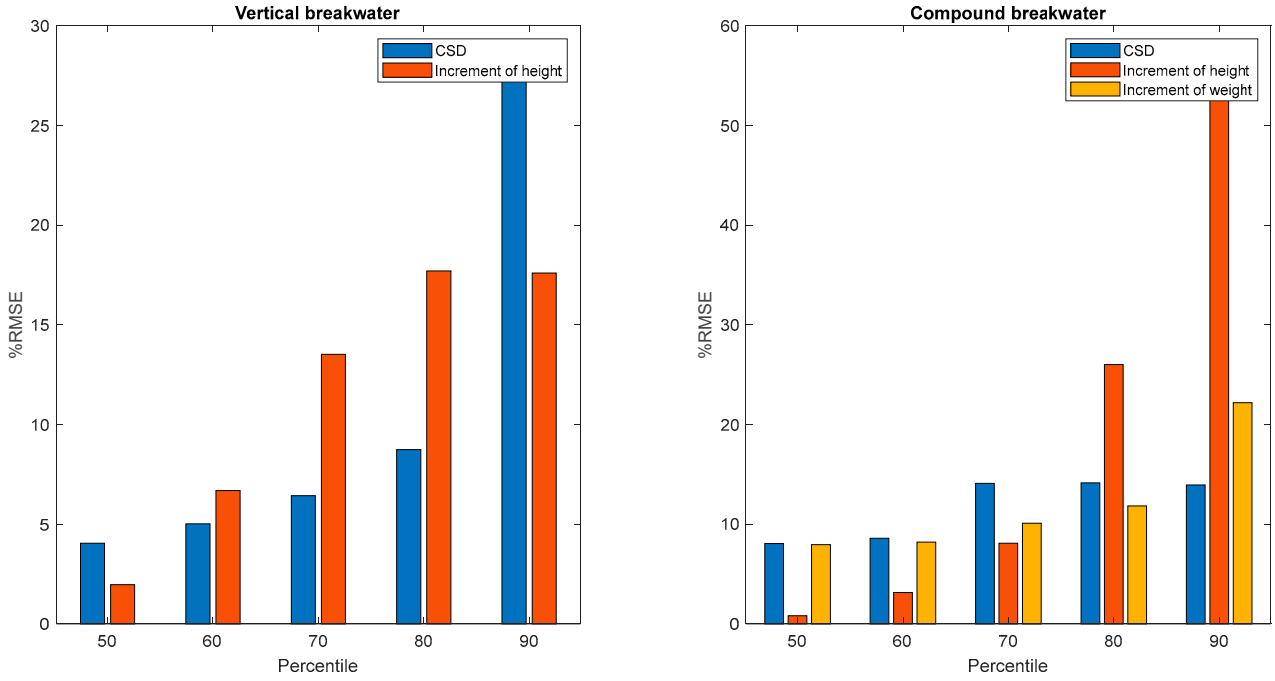

Figure 15. Distribution of the errors of the ANN-GA model.

Lastly, it is crucial to underscore the significance of adopting a probabilistic approach in climate change studies and incorporating the peak period consideration when assessing the safety of structures. In certain cases, the sea state associated with the highest wave height may not necessarily be the most destructive. The peak period assumes a pivotal role in the design of vertical and compound breakwaters, exerting considerable influence on their safety. Consequently, these variables demand important attention. Therefore, when scrutinizing the adaptation of such structures, it is imperative to embrace a probabilistic and non-deterministic approach, evaluating the impact of various sea states on the structure, with particular emphasis on diverse peak periods.

Regarding the limitations of the study, the ANN models were trained using outputs derived from established empirical formulations due to the lack of sufficiently extensive field measurements and laboratory experiments for the considered breakwater typologies and future climate scenarios. The use of full physics-based numerical models was not a viable alternative, as such models require very large amounts of input data, high computational effort, and are typically designed to resolve specific processes or structural components rather than the integrated response of an entire breakwater system. Implementing a fully coupled numerical model for the complete structure would therefore entail an impractical computational cost for the scope of this study. As a result, empirical equations constituted the only feasible and consistent basis to generate a sufficiently large and diverse dataset for AI training. An additional important limitation concerns the treatment of extreme events and outliers, as previously discussed. Improving AI performance for rare and extreme wave conditions requires dedicated methodological developments and extended datasets, which are beyond the scope of the present work.

4. Conclusions

Artificial intelligence is one of the leading technologies of our time, and across many scientific fields, AI-based and other data-driven models are emerging as strong alternatives

to traditional approaches. Although these methods have advanced rapidly in numerous areas, marine and coastal engineering has progressed more slowly. The potential of AI-driven models is considerable, offering gains in computational efficiency, accuracy, and overall performance. To avoid falling behind, the discipline must incorporate these tools and take advantage of their ability to improve modelling capabilities. This paper introduces an initial exploration of a novel AI-based methodology utilizing ANNs and GAs to tailor coastal structures for adaptation to climate change.

Numerous breakthroughs mark the evolution of this novel model. Foremost among these is the efficacy demonstrated by hybrid models employing a combination of diverse AI techniques and optimization algorithms. Traditionally, optimizing neural network models involved a resource-intensive trial-and-error methodology. However, the integration of optimization algorithms, such as GAs, has proven to result in a model development 30–40 times more efficient.

In the realm of coastal structure adaptation, models grow more intricate, involving a multitude of variables beyond the scope of predicting or propagating wave climate. This complexity significantly amplifies computational demands, underscoring the heightened importance of optimizing the parameters of these models. While ANNs already offer a computational advantage compared to numerical models, achieving an optimized model becomes paramount. A sensitivity analysis is essential to identify the variables that most effectively define the modelling process. The number of inputs must be minimized, as each additional input can escalate computational time by 15% to 50%, which means that in a model requiring a day for training, adding only one more input could translate to an additional half-day of computational effort.

Referring to the analysis of the errors of the model, it is important to notice that up to 60% of the total errors are concentrated in the 90th percentile of the distribution of the cases analyzed. The model performs less reliably at the extremes, so those situations deserve more careful review. The authors propose a critical examination of the modelling of extreme cases and emphasize the importance of meticulous data preprocessing to enhance the accuracy of predicting these outliers. Adequate inclusion of extreme data cases becomes imperative to mitigate significant errors and guarantee the precision of the model.

Future research should focus on improving data preprocessing strategies for training, validation, and testing in order to enhance ANN performance, particularly for extreme wave conditions. In addition, future studies should apply the proposed models using experimental and field data to further assess their robustness and capability to capture real wave–structure interaction processes.

In the specific context of the Valencia port study, it is recommended to raise the crown height by up to 1.2 m in the head section (vertical breakwater) and approximately 0.4 m in the stretch four of the trunk section (compound breakwater) to align both sections with the demands of climate change. In addition, a strengthening of the armor layer in the case of the compound breakwater would also be needed.

Author Contributions: Conceptualization, N.P.J., J.O.R., J.M.d.C., V.N.V. and P.T.; methodology, N.P.J., J.O.R., J.M.d.C., V.N.V. and P.T.; software, N.P.J., J.O.R. and P.T.; validation, N.P.J., J.O.R., J.M.d.C., V.N.V. and P.T.; formal analysis, N.P.J., J.O.R., J.M.d.C., V.N.V. and P.T.; investigation, N.P.J., J.O.R., J.M.d.C., V.N.V. and P.T.; resources, N.P.J., V.N.V. and P.T.; data curation, N.P.J. and J.O.R.; writing—original draft preparation, N.P.J. and J.O.R.; writing—review and editing, J.M.d.C., V.N.V. and P.T.; visualization, N.P.J., J.O.R., J.M.d.C., V.N.V. and P.T.; supervision, V.N.V. and P.T.; project administration, V.N.V. and P.T.; funding acquisition, N.P.J. and J.M.d.C. All authors have read and agreed to the published version of the manuscript.

Funding: This research received funding from Ministerio de Ciencia e Innovación of Spain. Nerea Portillo Juan received an FPU scholarship (FPU21/00812).

Data Availability Statement: Data used in this research can be found on the webpage www.puertos.es.

Conflicts of Interest: The authors declare no conflicts of interest.

References

1. Croquer, S.; Diaz-Carrasco, P.; Tamimi, V.; Poncet, S.; Lacey, J.; Nistor, I. Modelling wave-structure interactions including air compressibility: A case study of breaking wave impacts on a vertical wall along the Saint-Lawrence Bay. *Ocean Eng.* **2023**, *273*, 113971. [CrossRef]
2. Portillo Juan, N.; Negro Valdecantos, V.; del Campo, J.M. Review of the Impacts of Climate Change on Ports and Harbours and Their Adaptation in Spain. *Sustainability* **2022**, *14*, 7507. [CrossRef]
3. Xie, D.; Zou, Q.-P.; Mignone, A.; MacRae, J.D. Coastal flooding from wave overtopping and sea level rise adaptation in the northeastern USA. *Coast. Eng.* **2019**, *150*, 39–58. [CrossRef]
4. Ritphring, S.; Nidhinarangkoon, P.; Udo, K.; Shirakawa, H. The Comparative Study of Adaptation Measure to Sea Level Rise in Thailand. *J. Mar. Sci. Eng.* **2021**, *9*, 588. [CrossRef]
5. Luo, X.; Lin, T. Probabilistic Sea Level Rise Hazard Analysis Based on the Current Generation of Data and Protocols. *J. Struct. Eng.* **2023**, *149*, 04022252. [CrossRef]
6. Christodoulou, A.; Christidis, P.; Demirel, H. Sea-level rise in ports: A wider focus on impacts. *Marit. Econ. Logist.* **2019**, *21*, 482–496. [CrossRef]
7. Pau Sierra, J. Economic Impact of Overtopping and Adaptation Measures in Catalan Ports Due to Sea Level Rise. *Water* **2019**, *11*, 1440. [CrossRef]
8. Almar, R.; Ranasinghe, R.; Bergsma, E.W.J.; Diaz, H.; Melet, A.; Papa, F.; Vousdoukas, M.; Athanasiou, P.; Dada, O.; Almeida, L.P.; et al. A global analysis of extreme coastal water levels with implications for potential coastal overtopping. *Nat. Commun.* **2021**, *12*, 3775. [CrossRef]
9. Jin, Y.; Wang, W.; Kamath, A.; Bihs, H. Numerical Investigation on Wave-Overtopping at a Double-Dike Defence Structure in Response to Climate Change-Induced Sea Level Rise. *Fluids* **2022**, *7*, 295. [CrossRef]
10. Pau Sierra, J.; Casanovas, I.; Mosso, C.; Mestres, M.; Sanchez-Arcilla, A. Vulnerability of Catalan (NW Mediterranean) ports to wave overtopping due to different scenarios of sea level rise. *Reg. Environ. Change* **2016**, *16*, 1457–1468. [CrossRef]
11. Sierra, J.P.; Casas-Prat, M.; Virgili, M.; Moesso, C.; Sanchez-Arcilla, A. Impacts on wave-driven harbour agitation due to climate change in Catalan ports. *Nat. Hazards Earth Syst. Sci.* **2015**, *15*, 1695–1709. [CrossRef]
12. Sierra, J.P.; Genius, A.; Lionello, P.; Mestres, M.; Mosso, C.; Marzo, L. Modelling the impact of climate change on harbour operability: The Barcelona port case study. *Ocean Eng.* **2017**, *141*, 64–78. [CrossRef]
13. Romano-Moreno, E.; Diaz-Hernandez, G.; Tomás, A.; Lara, J.L. Multimodal harbor wave climate characterization based on wave agitation spectral types. *Coast. Eng.* **2023**, *180*, 104271. [CrossRef]
14. Camus, P.; Tomás, A.; Diaz-Hernandez, G.; Rodriguez, B.; Izaguirre, C.; Losada, I.J. Probabilistic assessment of port operation downtimes under climate change. *Coast. Eng.* **2019**, *147*, 12–24. [CrossRef]
15. Gracia, V.; Pau Sierra, J.; Gomez, M.; Pedrol, M.; Sampe, S.; Garcia-Leon, M.; Gironella, X. Assessing the impact of sea level rise on port operability using LiDAR-derived digital elevation models. *Remote Sens. Environ.* **2019**, *232*, 111318. [CrossRef]
16. Jebbad, R.; Sierra, J.P.; Mosso, C.; Mestres, M.; Sanchez-Arcilla, A. Assessment of harbour inoperability and adaptation cost due to sea level rise. Application to the port of Tangier-Med (Morocco). *Appl. Geogr.* **2022**, *138*, 102623. [CrossRef]
17. Izaguirre, C.; Losada, I.J.; Camus, P.; Vigh, J.L.; Stenek, V. Climate change risk to global port operations. *Nat. Clim. Change* **2021**, *11*, 14–20. [CrossRef]
18. Berman, M.; Baztan, J.; Kofinas, G.; Vanderlinden, J.-P.; Chouinard, O.; Huctin, J.-M.; Kane, A.; Mazé, C.; Nikulkina, I.; Thomson, K. Adaptation to climate change in coastal communities: Findings from seven sites on four continents. *Clim. Change* **2020**, *159*, 1–16. [CrossRef]
19. Maria Abadie, L.; Sainz de Murieta, E.; Galarraga, I. The Costs of Sea-Level Rise: Coastal Adaptation Investments vs. Inaction in Iberian Coastal Cities. *Water* **2020**, *12*, 1220. [CrossRef]
20. Hanson, S.E.; Nicholls, R.J. Demand for Ports to 2050: Climate Policy, Growing Trade and the Impacts of Sea-Level Rise. *Earths Future* **2020**, *8*, e2020EF001543. [CrossRef]
21. Sauer, I.J.; Roca, E.; Villares, M. Integrating climate change adaptation in coastal governance of the Barcelona metropolitan area. *Mitig. Adapt. Strateg. Glob. Change* **2021**, *26*, 16. [CrossRef]
22. Losada, I.J.; Toimil, A.; Muñoz, A.; Garcia-Fletcher, A.P.; Diaz-Simal, P. A planning strategy for the adaptation of coastal areas to climate change: The Spanish case. *Ocean Coast. Manag.* **2019**, *182*, 104983. [CrossRef]
23. Griggs, G.; Reguero, B.G. Coastal Adaptation to Climate Change and Sea-Level Rise. *Water* **2021**, *13*, 2151. [CrossRef]
24. Toimil, A.; Losada, I.J.; Nicholls, R.J.; Dalrymple, R.A.; Stive, M.J.F. Addressing the challenges of climate change risks and adaptation in coastal areas: A review. *Coast. Eng.* **2020**, *156*, 103611. [CrossRef]

25. Xuan, T.L.; Ba, H.T.; Thanh, V.Q.; Wright, D.P.; Tanim, A.H.; Anh, D.T. Evaluation of coastal protection strategies and proposing multiple lines of defense under climate change in the Mekong Delta for sustainable shoreline protection. *Ocean Coast. Manag.* **2022**, *228*, 106301. [CrossRef]
26. Sierra, J.P.; Garcia-Leon, M.; Gracia, V.; Sanchez-Arcilla, A. Green measures for Mediterranean harbours under a changing climate. *Proc. Inst. Civ. Eng. Marit. Eng.* **2017**, *170*, 55–66. [CrossRef]
27. Takagi, H.; Kashihara, H.; Esteban, M.; Shibayama, T. Assessment of future stability of breakwaters under climate change. *Coast. Eng. J.* **2011**, *53*, 21–39. [CrossRef]
28. Suh, K.-D.; Kim, S.-W.; Mori, N.; Mase, H. Effect of Climate Change on Performance-Based Design of Caisson Breakwaters. *J. Waterw. Port Coast. Ocean Eng. ASCE* **2012**, *138*, 215–225. [CrossRef]
29. Mase, H.; Tsujio, D.; Yasuda, T.; Mori, N. Stability analysis of composite breakwater with wave-dissipating blocks considering increase in sea levels, surges and waves due to climate change. *Ocean Eng.* **2013**, *71*, 58–65. [CrossRef]
30. Sekimoto, T.; Isobe, M.; Anno, K.; Nakajima, S. A new criterion and probabilistic approach to the performance assessment of coastal facilities in relation to their adaptation to global climate change. *Ocean Eng.* **2013**, *71*, 113–121. [CrossRef]
31. Lee, C.-E.; Kim, S.-W.; Park, D.-H.; Suh, K.-D. Risk assessment of wave run-up height and armor stability of inclined coastal structures subject to long-term sea level rise. *Ocean Eng.* **2013**, *71*, 130–136. [CrossRef]
32. Sergent, P.; Prevot, G.; Mattarolo, G.; Brossard, J.; Morel, G.; Mar, F.; Benoit, M.; Ropert, F.; Kergadallan, X.; Trichet, J.-J.; et al. Adaptation of coastal structures to mean sea level rise. *Houille Blanche* **2014**, *100*, 54–61. [CrossRef]
33. Formentin, S.M.; Palma, G.; Zanuttigh, B. Integrated assessment of the hydraulic and structural performance of crown walls on top of smooth berms. *Coast. Eng.* **2021**, *168*, 103951. [CrossRef]
34. Allsop, W. Climate Change Threats to Two Breakwaters. *J. Mar. Sci. Eng.* **2022**, *10*, 1613. [CrossRef]
35. Radfar, S.; Galiatsatou, P. Influence of nonstationarity and dependence of extreme wave parameters on the reliability assessment of coastal structures—A case study. *Ocean Eng.* **2023**, *273*, 113862. [CrossRef]
36. Baldoni, A.; Marini, F.; Filomena, G.; Parlani, S.; Brocchini, M. Climate change-driven coastal flooding in the Mid Adriatic Sea and adaptation of coastal defense structures. *Estuar. Coast. Shelf Sci.* **2025**, *326*, 109535. [CrossRef]
37. Tomas, A.; Alvarez de Eulate, M.; Barajas, G.; Lara, J.; Losada, I.; Segovia, M.; Esteban, F. A New Methodology to Simulate Three-Dimensional Hydraulic Loads on a Vertical Breakwater along its Life Cycle. In *Coastal Structures 2019*; Bundesanstalt für Wasserbau: Karlsruhe, Germany, 2019.
38. Lucio, D.; Lara, J.; Tomas, A.; Losada, I.J. Probabilistic hydraulic design of non-conventional breakwaters in shallow water conditions. In *Coastal Structures 2019*; Bundesanstalt für Wasserbau: Karlsruhe, Germany, 2019.
39. Suzuki, T.; Garcia-Feal, O.; Dominguez, J.M.; Altomare, C. Simulation of 3D overtopping flow-object-structure interaction with a calibration-based wave generation method with DualSPHysics and SWASH. *Comput. Part. Mech.* **2022**, *9*, 1003–1015. [CrossRef]
40. Portillo Juan, N.; Olalde Rodríguez, J.; Negro Valdecantos, V.; Iglesias, G. Data-driven and physics-based approach for wave downscaling: A comparative study. *Ocean Eng.* **2023**, *285*, 115380. [CrossRef]
41. Portillo Juan, N.; Negro Valdecantos, V. Review of the application of Artificial Neural Networks in ocean engineering. *Ocean Eng.* **2022**, *259*, 111947. [CrossRef]
42. Portillo Juan, N.; Negro Valdecantos, V.; del Campo, J.M. Analysis of Monthly Recorded Climate Extreme Events and Their Implications on the Spanish Mediterranean Coast. *Water* **2022**, *14*, 3453. [CrossRef]
43. Puertos del Estado. Oceanografía. Registros Históricos de Oleaje. Updated 19 September 2022. Available online: https://www.puertos.es/es-es/oceanografia/Paginas/portus.aspxInicio%7CPuertos (accessed on 23 September 2022).
44. Grau, J.I.; Burgos, M.A.; Barquín, G.G.; Carvajal, A.L.; Albiach, J.C.C. *Diques de Abrigo en los Puertos de Interés General del Estado*; Ministerio de Fomento: Madrid, Spain, 2012.
45. Goda, Y. (Ed.) *A Synthesis of Breaker Indices*; Japan Society of Civil Engineers: Tokyo, Japan, 1970.
46. Goda, Y. Irregular Wave Deformation in the Surf Zone. *Coast. Eng. Jpn.* **1975**, *18*, 13–26. [CrossRef]
47. van der Meer, J. (Ed.) *Rock Slopes and Gravel Beaches Under Wave Attack*; Delft Hydraulics: Delft, The Netherlands, 1988.
48. Goda, Y. *Random Seas and Design of Maritime Structures*; World Scientific Publishing Company: Singapore, 2010.
49. van der Meer, J.; Regeling, H.; Waal, J. Wave Transmission: Spectral Changes and Its Effects on Run-Up and Overtopping. In *Coastal Engineering 2000—Proceedings of the 27th International Conference on Coastal Engineering, ICCE 2000*; American Society of Civil Engineers: Sydney, Australia, 2000; Volume 276.
50. van der Meer, J.; Allsop, W.; Bruce, T.; Rouck, J.; Kortenhaus, A.; Pullen, T.; Schüttrumpf, H.; Troch, P.; Zanuttigh, B. *EurOtop: Manual on Wave Overtopping of Sea Defences and Related Structures—An Overtopping Manual Largely Based on European Research, but for Worlwide Application*, 2nd ed.; HR Wallingford: Wallingford, UK, 2016.
51. Franco, L.; Gerloni, M.d.; Meer, J.v.d. (Eds.) *Wave Overtopping on Vertical and Composite Breakwaters*; American Society of Civil Engineers: Kobe, Japan, 2010.
52. Allsop, W.; Hettiarachchi, S. *Wave Reflections in Harbours: Design, Construction and Performance of Wave Absorbing Structures*; Hydraulics Research Limited: Wallingford, UK, 1989.

53. Juan Nerea, P.; Rodríguez Javier, O.; Valdecantos Vicente, N. Comparison of the SIMAR-WANA, ERA-5, and Waverys Databases for Maritime Climate Estimations and the Implications of Coastal Protection Structures. *J. Waterw. Port Coast. Ocean. Eng.* **2024**, *150*, 04023021. [CrossRef]
54. Goda, Y. Performance-Based Design of Caisson Breakwaters with New Approach to Extreme Wave Statistics. *Coast. Eng. J.* **2001**, *43*, 289–316. [CrossRef]
55. Medina, J.R.; Garrido, J.M.; Gómez-Martín, M.E.; Vidal, C. Armor Damage Analysis Using Neural Networks. In *Coastal Structures 2003*; American Society of Civil Engineers: Portland, OR, USA, 2004; pp. 236–248.
56. Portillo Juan, N.; Matutano, C.; Negro Valdecantos, V. Uncertainties in the application of artificial neural networks in ocean engineering. *Ocean Eng.* **2023**, *284*, 115193. [CrossRef]
57. MathWorks. *MATLAB*, version 9.11.0 (R2021b); The MathWorks Inc.: Natick, MA, USA, 2021.
58. Holland, J.H. Genetic Algorithms. *Sci. Am.* **1992**, *267*, 66–73. [CrossRef]
59. Katoch, S.; Chauhan, S.S.; Kumar, V. A review on genetic algorithm: Past, present, and future. *Multimed. Tools Appl.* **2021**, *80*, 8091–8126. [CrossRef]
60. Wang, B.; Wang, B.; Wu, W.; Xi, C.; Wang, J. Sea-water-level prediction via combined wavelet decomposition, neuro-fuzzy and neural networks using SLA and wind information. *Acta Oceanol. Sin.* **2020**, *39*, 157–167. [CrossRef]
61. Yedjour, D.; Benyettou, A.; Yedjour, H. Symbolic interpretation of artificial neural networks using genetic algorithms. *Turk. J. Electr. Eng. Comput. Sci.* **2018**, *26*, 2465–2475. [CrossRef]